

Supplementary Information

Unraveling the Faradaic Electrochemical Efficiencies over Fe/Co Spinel Metal Oxides using Surface Spectroscopy and Microscopy Techniques.

Varchaswal Kashyap,^{a, b} Ajmal Pandikassala,^{a, b} Gourav Singla,^a Tuhin Suvra Khan,^{*,c} M. Ali Haider,^d C. P. Vinod,^{*,b, e} and Sreekumar Kurungot^{*,a, b}

^a Physical and Materials Chemistry Division, CSIR-National Chemical Laboratory, Dr. Homi Bhabha Road, Pune 41108, India.

^b Academy of Scientific and Innovative Research, Postal Staff College Area, Kamla Nehru Nagar, Ghaziabad, Uttar Pradesh-201002, India.

^c Nanocatalysis Area, Light Stock Processing Division, CSIR-Indian Institute of Petroleum, Dehradun 248005, Uttarakhand, India.

^d Renewable Energy and Chemicals Laboratory, Department of Chemical Engineering, Indian Institute of Technology Delhi, Hauz Khas, Delhi 110016, India.

^e Catalysis and Inorganic Chemistry Division, CSIR-National Chemical Laboratory, Dr. Homi Bhabha Road, Pune 41108, India.

Email: k.sreekumar@ncl.res, cp.vinod@ncl.res.in, tuhin.khan@iip.res.in

Calculation of Work function(φ_m):

$$\varphi_m = h\nu - W$$

where, h = plank constant, ν = frequency of photon; here, $h\nu = 21.2$ eV; W = width of the emitted photoelectron's peak from the UPS spectrum.

Work function (φ_m) for Co_3O_4 (φ_1) = 5.6 eV; Fe_2O_3 (φ_2) = 6.1 eV; Co_2FeO_4 (φ_3) = 6.2 eV; CoFe_2O_4 (φ_4) = 6.3 eV.

Conduction Band (CB.) and Valence Band (VB): For the calculation of the conduction band (CB) and valence band (VB), the following formulae were used as reported previously in the literature ¹⁻⁴:

$$E_{CB} = \chi - E_c - \frac{1}{2}E_g$$

$$E_{VB} = E_{CB} + E_g$$

where, E_{CB} is the energy of CB, E_c is the energy of the free electron, E_g is the bandgap of the semiconductor and E_{VB} is the energy of VB. Also, χ represents the absolute electronegativity of the semiconducting material in the Mulliken electronegativity. The detailed calculations of the various nanocomposites are as follows:

First ionization energy of cobalt = 760.4 kJ/mol = 760.4/96.48 = 7.88 eV

First ionization energy of iron = 762.5 kJ/mol = 762.5/96.48 = 7.90 eV

Electron affinity of cobalt = 63.7 kJ/mol = 63.7/96.48 = 0.66 eV

Electron affinity of iron = 15.7 kJ/mol = 15.7/96.48 = 0.16 eV

$$\chi_{Co} = \frac{(EA + E_{ion})}{2} = \frac{(0.66 + 7.88)}{2} = 4.27 \text{ eV}$$

$$\chi_{Fe} = \frac{(EA + E_{ion})}{2} = \frac{(0.16 + 7.90)}{2} = 4.03 \text{ eV}$$

$\chi_0 = 7.49$ eV; $\chi_{\text{Co}_3\text{O}_4} = 5.88$ eV; $\chi_{\text{Co}_2\text{FeO}_4} = 5.83$ eV; $\chi_{\text{CoFe}_2\text{O}_4} = 5.79$ eV; $\chi_{\text{Fe}_2\text{O}_3} = 5.84$ eV

Co₃O₄ $E_{CB} = \chi_{\text{Co}_3\text{O}_4} - E_c - \frac{1}{2}(E_{g,\text{Co}_3\text{O}_4}) = 5.88 - 4.5 - 1.15 = 0.23 \text{ eV}$

$$E_{VB} = E_{CB} + E_{g,\text{Co}_3\text{O}_4} = 0.23 + 2.3 = 2.53 \text{ eV}$$

$$\underline{\text{Co}_2\text{FeO}_4} \quad E_{CB} = \chi_{\text{Co}_2\text{FeO}_4} - E_c - \frac{1}{2}(E_{g,\text{Co}_2\text{FeO}_4}) = 5.83 - 4.5 - 1.25 = 0.08 \text{ eV}$$

$$E_{VB} = E_{CB} - E_{g,\text{Co}_2\text{FeO}_4} = 0.08 + 2.5 = 2.58 \text{ eV}$$

$$\underline{\text{CoFe}_2\text{O}_4} \quad E_{CB} = \chi_{\text{CoFe}_2\text{O}_4} - E_c - \frac{1}{2}(E_{g,\text{CoFe}_2\text{O}_4}) = 5.79 - 4.5 - 1.4 = -0.11 \text{ eV}$$

$$E_{VB} = E_{CB} - E_{g,\text{CoFe}_2\text{O}_4} = -0.11 + 2.8 = 2.69 \text{ eV}$$

$$\underline{\text{Fe}_2\text{O}_3} \quad E_{CB} = \chi_{\text{Fe}_2\text{O}_3} - E_c - \frac{1}{2}(E_{g,\text{Fe}_2\text{O}_3}) = 5.84 - 4.5 - 1.1 = 0.24 \text{ eV}$$

$$E_{VB} = E_{CB} - E_{g,\text{Fe}_2\text{O}_3} = 0.24 + 2.2 = 2.44 \text{ eV}$$

Catalyst Slurry Preparation:

Catalyst slurry for HER and OER: 2 mg of the catalyst was dispersed in 1 ml of 3:2 water:isopropyl solution. Subsequently, 40 μl of 5 wt. % Nafion solution was added as the binder. The dispersion was made feasible through ultra-sonication of the sample for 30 min. As such prepared catalyst slurry was drop coated on the glassy carbon electrode (geometrical surface area: 0.07 cm^2), which was subsequently dried at room temperature.

Catalyst slurry for ORR: In a typical process, 2 mg of the catalyst along with 8 mg of Vulcan carbon and 40 μl of the 5 wt. % Nafion solution were dispersed in 1 ml of water:isopropyl alcohol (3:2 v/v) mixture by ultra-sonicating for 1 h. 10 μl of the catalyst slurry was coated over the surface of the glassy carbon electrode (geometrical surface area: 0.196 cm^2). The electrode was dried at room temperature and subjected for the electrochemical studies.

Rotating Ring Disk Electrode Study:

The Rotating Ring Disc Electrode (RRDE) technique was used for estimating the percentage of H_2O_2 formed and the number of electrons transferred during the ORR process. A Pt ring (0.1866 cm^2) surrounded glassy carbon disc electrode of an area of 0.2475 cm^2 was used as the working electrode by keeping the ring potential at 0.60 V (V vs Hg/HgO). Hg/HgO was used as the reference electrode and a graphite rod was used as the counter electrode in the studies. This analysis has been performed in O_2 saturated 0.1 M KOH solution.

The mathematical equations used for the RRDE analysis are given below:

$$H_2O_2(\%) = 200 \times \frac{I_r}{I_d + \frac{I_r}{N}}$$

$$n = 4 \times \frac{I_d}{I_d + \frac{I_r}{N}}$$

where,

I_r - Ring current

I_d - Disc current

N - Collection efficiency of the ring electrode (0.37)

n - No of electrons

Calculation of bandgap from UV-visible absorption spectra:

The band gap is calculated by UV- Visible spectroscopy using the Tauc plot. By plotting the graph between $(\alpha h\nu)^{\frac{1}{n}}$ vs. photon energy $(h\nu)$.⁵

where,

α - optical absorption coefficient

h - Plank's constant

ν - Frequency

n - Power factor ($n= 0.5$ for direct transitions)

The energy band gap value is calculated by extrapolating the straight-line part of the curves to the zero-absorption coefficient value.

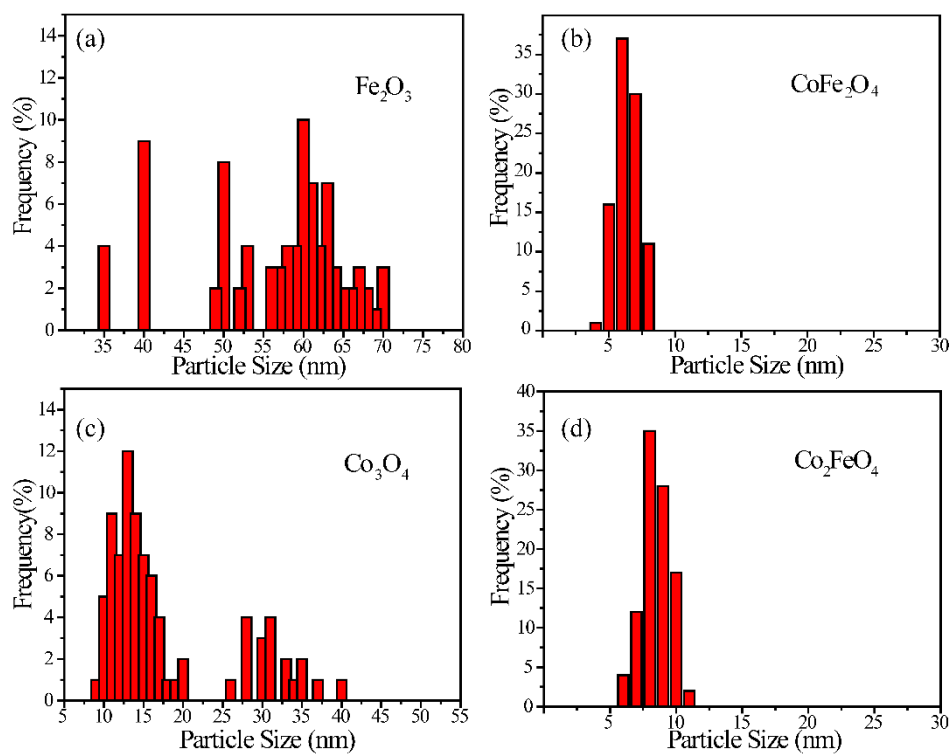


Fig. S1. The particle size distribution profiles of Fe_2O_3 (a), CoFe_2O_4 (b), Co_3O_4 (c), and Co_2FeO_4 (d) as calculated from the TEM analysis.

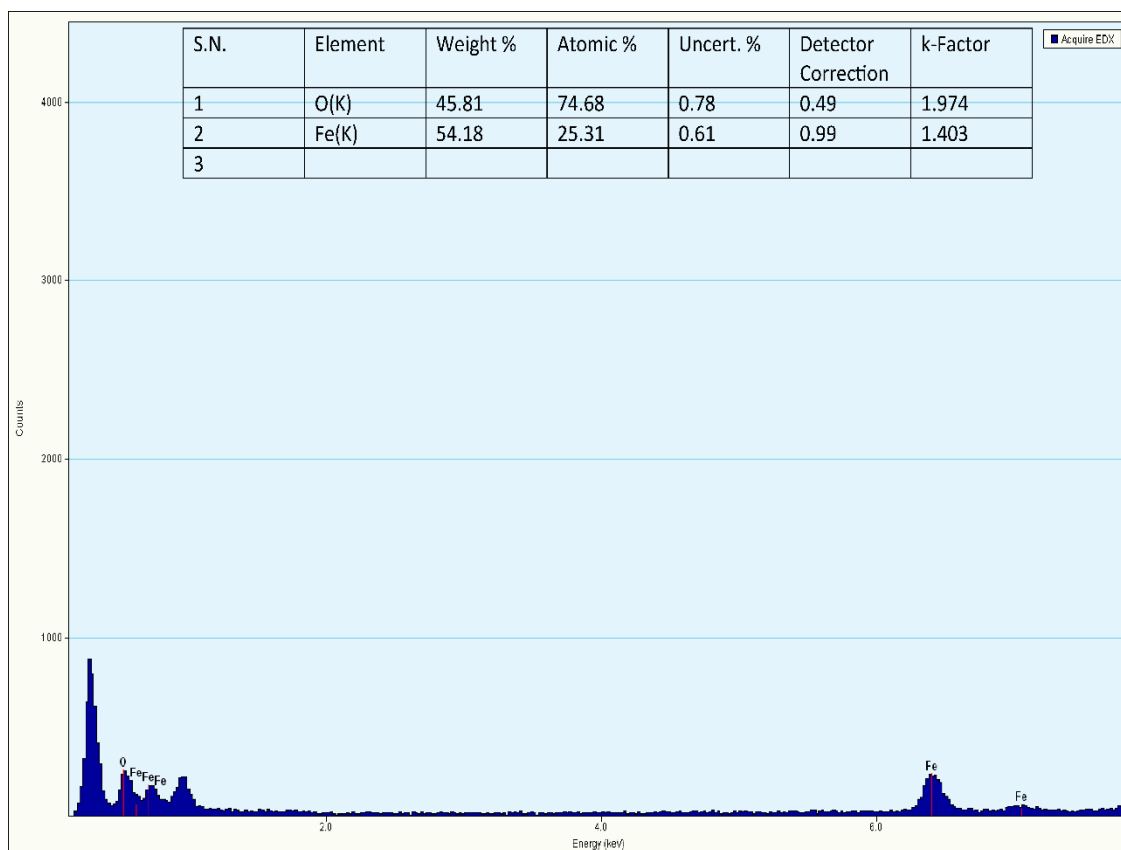


Fig. S2. EDAX of the Fe₂O₃ nanoparticles.

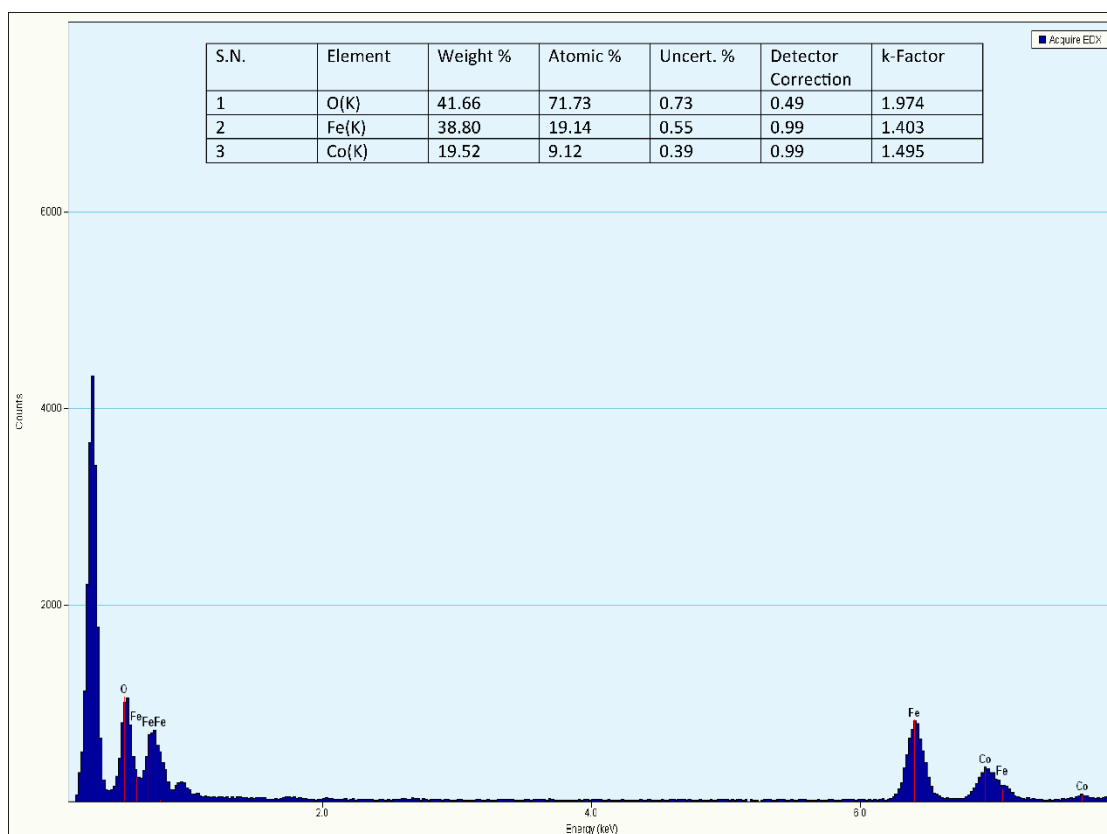


Fig. S3. EDAX of CoFe₂O₄ nanoparticles.

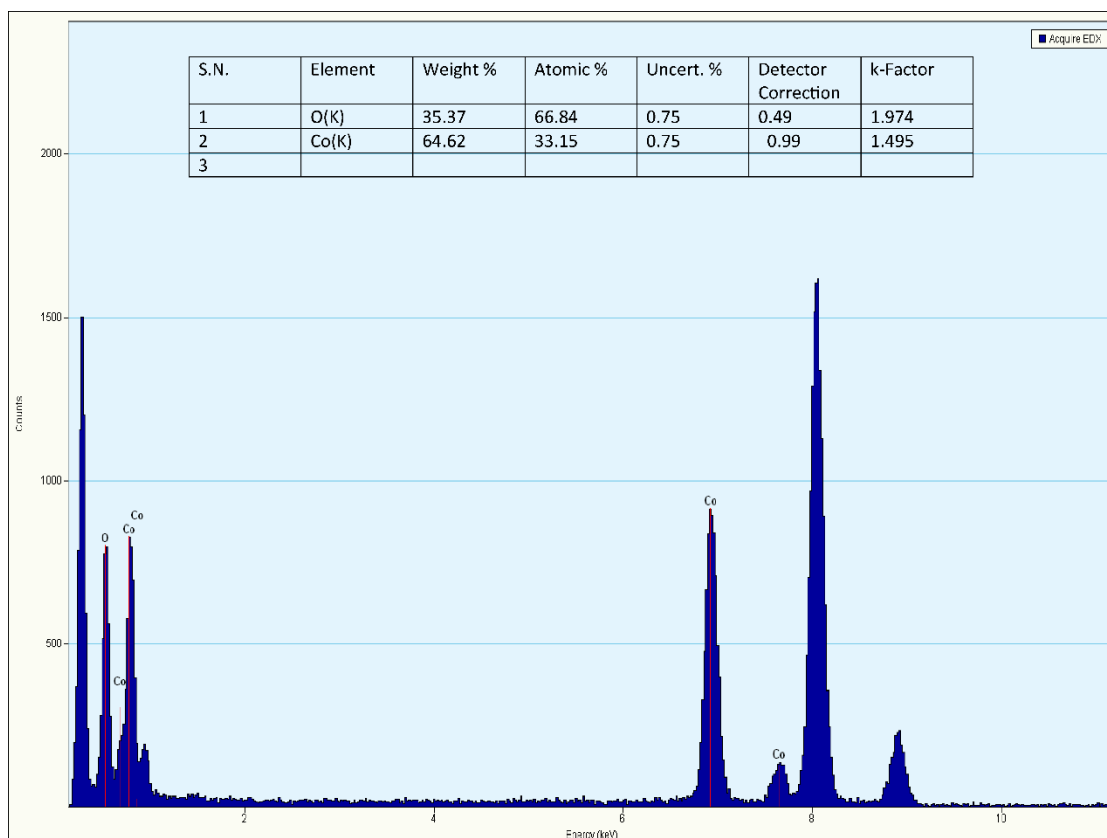


Fig. S4. EDAX of Co_3O_4 nanoparticles.

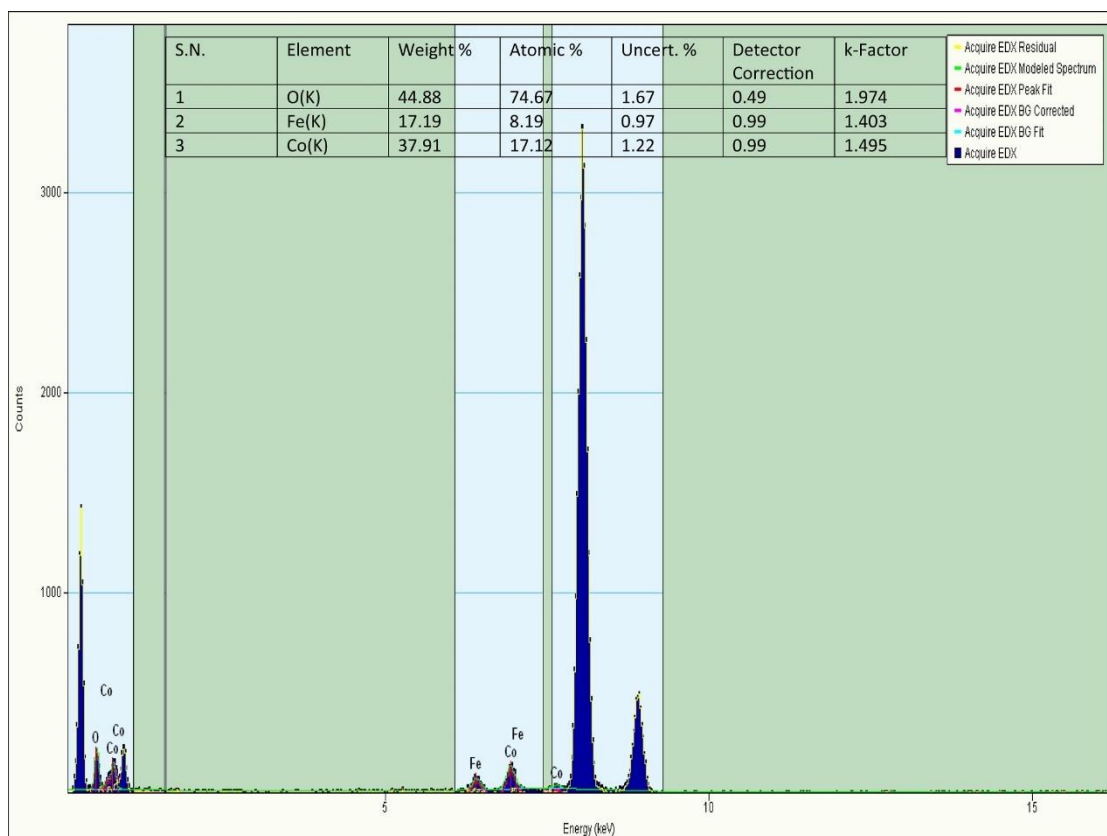


Fig. S5. EDAX of Co_2FeO_4 nanoparticles.

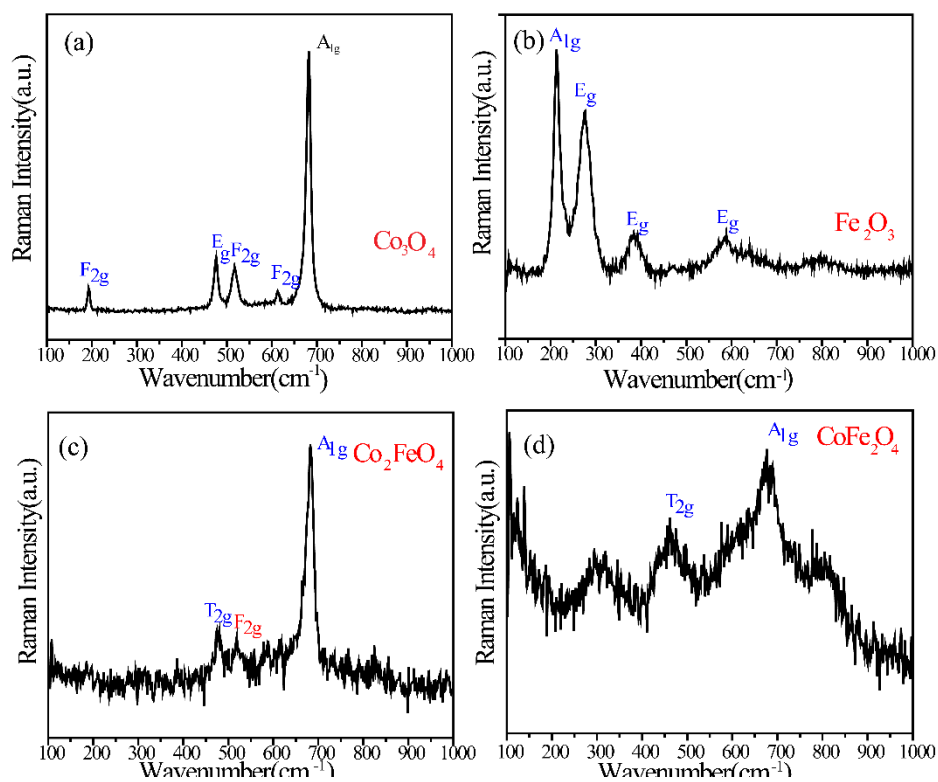


Fig. S6. Raman spectra of Co_3O_4 (a), Fe_2O_3 (b), Co_2FeO_4 (c), and CoFe_2O_4 (d).

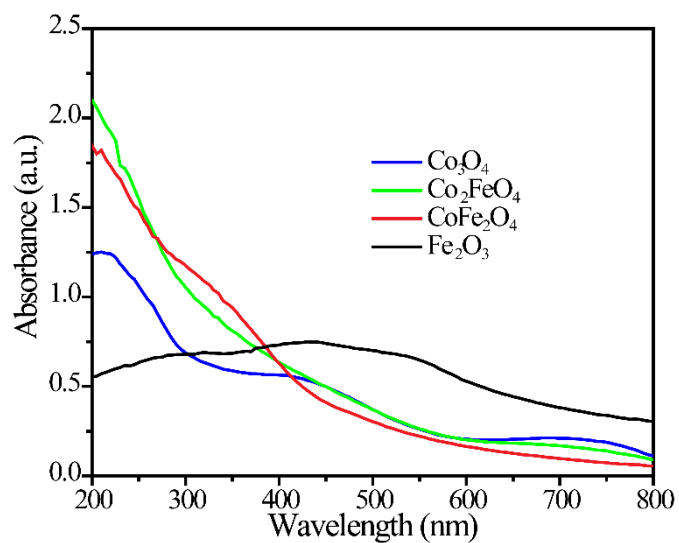


Fig. S7. UV-Visible spectra of the Fe_2O_3 , CoFe_2O_4 , Co_3O_4 and Co_2FeO_4 recorded using the water:ethanol solvent mixture.

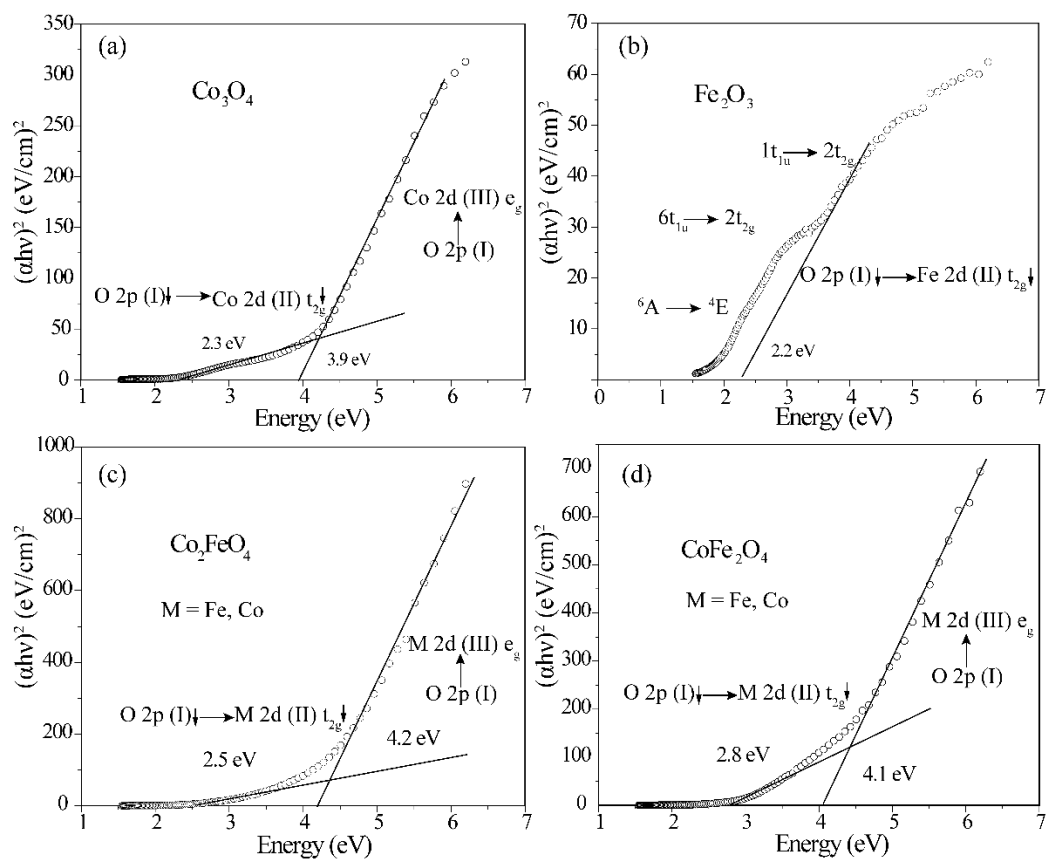


Fig. S8. Tauc plot of the Co_3O_4 , Fe_2O_3 , Co_2FeO_4 , and CoFe_2O_4 nanoparticles.⁶⁻⁹

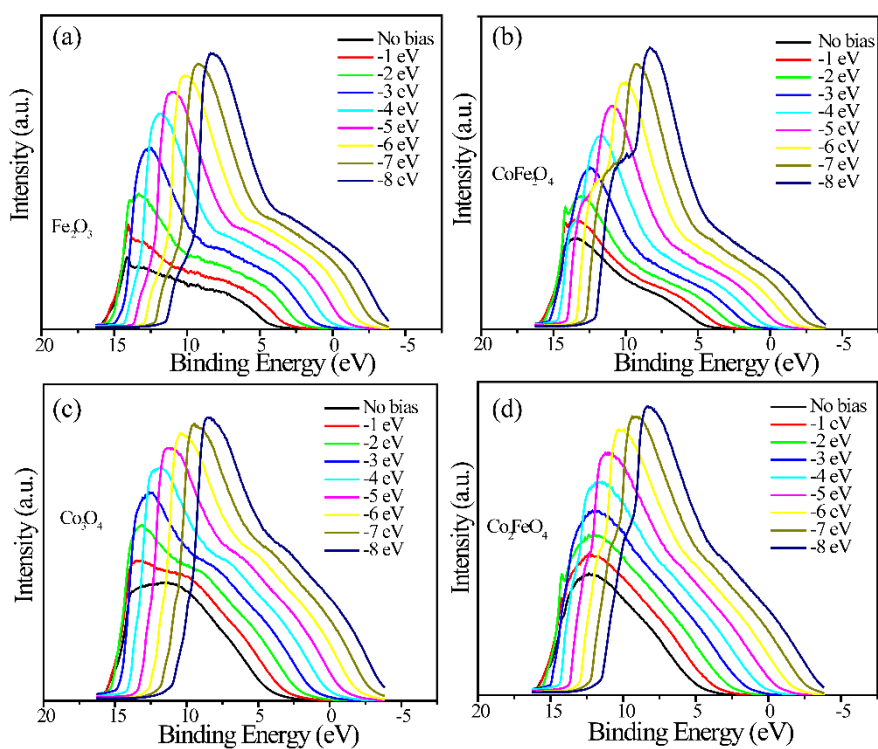


Fig. S9. Ultraviolet photoelectron spectra (UPS) of the Fe_2O_3 , CoFe_2O_4 , Co_2FeO_4 and Co_3O_4 nanoparticles.

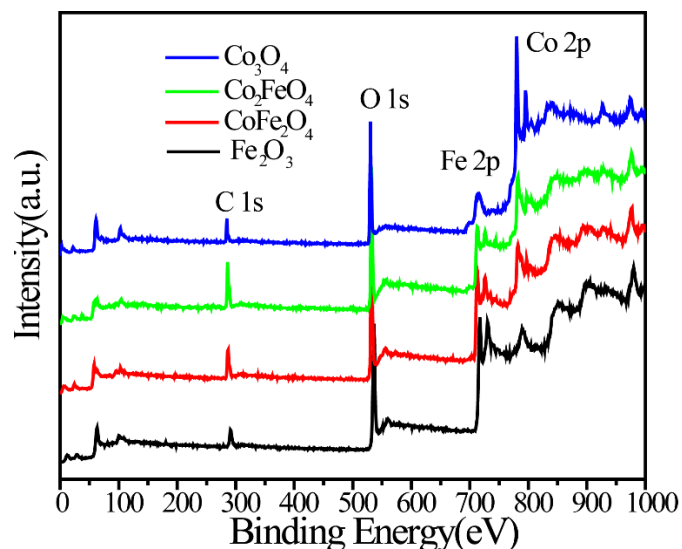


Fig. S10. Survey spectra of Co_3O_4 , Co_2FeO_4 , CoFe_2O_4 and Fe_2O_3 .

Table S1. Deconvoluted O 1s peak parameters of the Co_3O_4 , Co_2FeO_4 , CoFe_2O_4 and Fe_2O_3 nanoparticles.

| S.N. | Nanoparticle | Peak | O_L | O_V | O_C |
|------|---------------------------|----------|----------------------|----------------------|----------------------|
| 1 | Co_3O_4 | position | 529.9 | 531.5 | 532.8 |
| | | height | 145616.9 | 48842.8 | 10498.7 |
| | | width | 1.1 | 1.5 | 1.2 |
| | | Area (%) | 185701.4 (66.3 %) | 78023.0 (27.8 %) | 16050.3 (5.7 %) |
| 2 | Co_2FeO_4 | position | 530.8 | 532.3 | 533.0 |
| | | height | 130563.5 | 80129.0 | 33767.8 |
| | | width | 1.7 | 1.5 | 2.1 |
| | | area | 242879.2 (54.2 %) | 125254.9 (27.9 %) | 79972.4 (17.8 %) |
| 3 | CoFe_2O_4 | position | 530.68 | 531.9 | 533.0 |
| | | height | 119651.1 | 83609.2 | 29957.8 |
| | | width | 1.7 | 2 | 2.5 |
| | | area | 218238.6 (45.8 %) | 179425.7 (37.7 %) | 78060.6 (16.4 %) |
| 4 | Fe_2O_3 | position | 529.4 | 530.9 | 532.1 |
| | | height | 229202.7 | 64652.0 | 22786.5 |
| | | width | 1.2 | 1.4 | 2.0 |
| | | area | 341243.8 (70.2 %) | 96260.6 (19.8 %) | 484899.4 (10.0 %) |

Table S2. Deconvolute Co 2p and Fe 2p peak parameters of the Co_3O_4 , Co_2FeO_4 , CoFe_2O_4 and Fe_2O_3 nanoparticles.

| S.N. | Metal Oxide | 2p _{3/2} (eV) | | 2p _{1/2} (eV) | | Satellite 1 (eV) | Satellite 2 (eV) |
|------|----------------------------------|------------------------|---|------------------------|---|---|---|
| 1 | Co ₃ O ₄ | Co ³⁺ | 779.8 (A=162432; W=1.6; H=94335.8) | Co ³⁺ | 794.8 (A=58622.2; W=1.6; H=36601.1) | 786.5 (A=18545.3; W=2.5; H=5260.4) | 803.6 (A=21249.3; W=2; H=7340.8) |
| | | Co ²⁺ | 781.3 (A=296790.3; W=2.7; H=76977.4) | Co ²⁺ | 796.5 (A=83990.1; W=2.5; H=30701.8) | 789.5 (A=17717.8; W=2.3; H=6642.3) | 805.5 (A=6996.9; W=1.9; H=3517.2) |
| 2 | Co ₂ FeO ₄ | Co ³⁺ | 780.0 (A=147928.7; W=2.5; H=50338.7) | Co ³⁺ | 795.8 (A=39840.6; W=2.5; H=14955.3) | 784.7 (A=59912.2; W=3.7; H=15158.6) | 802.1 (A=34540.3; W=3.2; H=7980.0) |
| | | Co ²⁺ | 782.1 (A=65762.2; W=2.6; H=23860.3) | Co ²⁺ | 797.5 (A=35424.9; W=2.8; H=9496.3) | 787.6 (A=67604.5; W=4.7; H=13521.2) | 804.6 (A=19091.8; W=3.7; H=4250.5) |
| | | Fe ²⁺ | 710.7 (A=135327.8; W=2.8; H=45106.4) | Fe ²⁺ | 723.8 (A=63302.9; W=3.2; H=14049.2) | 718.2 (A=68578.4; W=5.1; H=12185.5) | 733.0 (A=11242.4; W=2.5; H=3163.0) |
| | | Fe ³⁺ | 713.2 (A=121275.1; W=3.7; H=26984.0) | Fe ³⁺ | 725.7 (A=48100.8; W=3.9; H=9787.6) | | |
| 3 | CoFe ₂ O ₄ | Co ³⁺ | 780.0 (A=128710.9; W=2.5; H=41233.0) | Co ³⁺ | 795.5 (A=41521.4; W=2.8; H=10600.5) | 785.1 (A=70420.3; W=3.9; H=16997.7) | 801.9 (A=28754.9; W=3.8; H=5522.7) |
| | | Co ²⁺ | 782.1 (A=81191.2; W=3.0; H=25227.6) | Co ²⁺ | 796.7 (A=21976.7; W=2.5; H=8258.3) | 788.0 (A=90033.4; W=5.2; H=15395.7) | 803.4 (A=19170.9; W=3.4; H=4106.1) |
| | | Fe ²⁺ | 710.7 (A=224118.9; W=2.9; H=71866.5) | Fe ²⁺ | 724.0 (A=126612.9; W=3.5; H=28959.8) | 718.4 (A=105608.0; W=5.2; H=19325.6) | 732.7 (A=20947.2; W=3.8 H=4672.3) |
| | | Fe ³⁺ | 713.5 (A=133193.4; W=3.4; H=33981.2) | Fe ³⁺ | 726.5 (A=66133.7; W=3.9; H=12939.2) | | |
| 4 | Fe ₂ O ₃ | Fe ²⁺ | 709.1 (A=243638.9; W=2.5; H=91565.8) | Fe ²⁺ | 722.7 (A=146835.2; W=3.0; H=38769.2) | 716.9 (A=161404.6; W=6.6; H=22815.4) | 731.1 (A=40813.6; W=4.5; H=8498.8) |

| | | | | | | | |
|--|--|------------------|---|------------------|---|--|--|
| | | Fe ³⁺ | 711.4 (A=174102.9; W=3.2; H=49390.3) | Fe ³⁺ | 725.0 (A=104031.7; W=4; H=21140.7) | | |
|--|--|------------------|---|------------------|---|--|--|

Table S3. Bandgap (E_g), conduction band (CB), valence band (VB) and work function (ϕ) values of the Co₃O₄, Co₂FeO₄, CoFe₂O₄ and Fe₂O₃ nanoparticles. (Diff. OER: Potential difference from oxygen electrode potential; Diff. ORR: Potential difference from oxygen reduction electrode potential).

| S.N. | Metal Oxide | Band Gap (eV) | C B (V vs NHE) | VB (V vs NHE) | Work function (ϕ) (eV) |
|------|----------------------------------|---------------|----------------------------------|---------------------------------|-------------------------------|
| 1 | Co ₃ O ₄ | 2.3 | 0.23 (Diff. OER*: ~ 1.0 eV) | 2.53 (Diff. ORR*: ~ 1.3 eV) | 5.6 |
| 2 | Co ₂ FeO ₄ | 2.6 | 0.08 (Diff. OER*: ~ 1.15 eV) | 2.58 (Diff. ORR*: ~ 1.35 eV) | 6.2 |
| 3 | CoFe ₂ O ₄ | 2.8 | -0.11 (Diff. OER*: ~ 1.34 eV) | 2.69 (Diff. ORR*: ~ 1.46 eV) | 6.3 |
| 4 | Fe ₂ O ₃ | 2.2 | 0.24 (Diff. OER*: ~ 0.9 eV) | 2.44 (Diff. ORR*: ~ 1.21 eV) | 6.1 |

DFT Method:

Plane-wave density functional theory (DFT) calculations as implemented in Vienna ab initio simulation package (VASP-5.3.5 version) were performed to calculate the oxygen vacancy formation energy for the Co₃O₄ and CoFe₂O₄ catalysts.¹⁰ Projector augmented wave method (PAW) was used for describing the interactions between the electrons and ions.¹¹ An energy cut-off of 396 eV was applied for truncating the plane-wave basis set. Perdew-Burke-Ernzerhof (PBE) exchange-correlation function developed by Perdew *et al.*, was used for all the DFT calculations.¹² Spin-polarized set-up was used, along with Hubbard U_{eff} parameters for Co and Fe of value 3.32 eV and 5.3 eV, respectively.¹³⁻¹⁴ The CoFe₂O₄ crystal geometry was obtained from the materials project database, whereas the Co₃O₄ crystal was obtained by replacing the

Fe with Co and performing lattice parameter optimization.¹⁵ Subsequently, the Co_3O_4 and CoFe_2O_4 bulk crystals were cleaved along the (001) direction to obtain the $\text{Co}_3\text{O}_4(001)$ and $\text{CoFe}_2\text{O}_4(001)$ surfaces. The $\text{Co}_3\text{O}_4(001)$ and $\text{CoFe}_2\text{O}_4(001)$ surface 3×3 supercell slabs were modelled using a slab of four Co(III)/Fe(III) atomic layers and three Co(II) atomic layers, having chemical formula $\text{Co(II)}_6\text{Co(III)}_{16}\text{O}_{32}$ and $\text{Co(II)}_6\text{Fe(III)}_{16}\text{O}_{32}$, as shown in Fig. S6. Both the bare $\text{Co(II)}_6\text{Co(III)}_{16}\text{O}_{32}$ and $\text{Co(II)}_6\text{Fe(III)}_{16}\text{O}_{32}$ (001) surface slabs have an overall formula charge of - 4. In order to balance the formal charge and to mimic the experimental OER condition, both the top and bottom surfaces of the $\text{Co}_3\text{O}_4(001)$ and $\text{CoFe}_2\text{O}_4(001)$ surface slabs were modified with 4H^+ , 2OH^- and $2\text{H}_2\text{O}$, as has been suggested by Plaisance *et al.*¹⁶ The $\text{Co}_3\text{O}_4(001)$ and $\text{CoFe}_2\text{O}_4(001)$ surfaces have been shown in Fig. 9(a) and 9(b). Monkhorst-Pack k-point mesh of $2 \times 2 \times 1$ and Gaussian smearing of 0.01 eV was used.¹⁷ For all the geometry optimization calculations, the bottom four atomic layers were kept fixed to their bulk configurations.

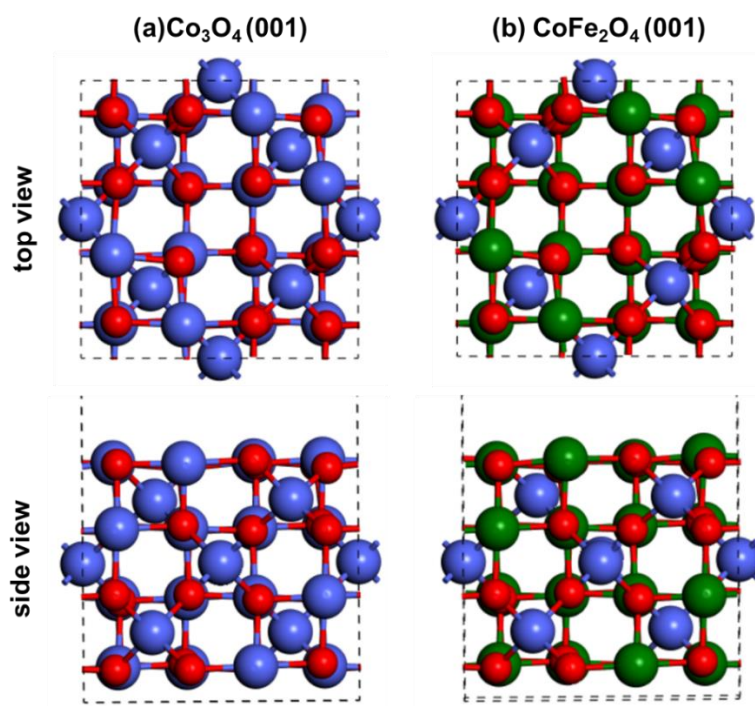


Fig. S11. $\text{Co}_3\text{O}_4(001)$ and $\text{CoFe}_2\text{O}_4(001)$ surfaces as cleaved from bulk geometry. Color code: Co (blue), Fe (green), O (red) and H (white).

References:

1. Y. Xu and M. A. A. Schoonen, *Am. Min.* **2000**, 85, 543-556.
2. S. Asadzadeh-Khaneghah and A. Habibi-Yangjeh, *J. Clean. Prod.* **2020**, 276, 124319.
3. M. Pirhashemi, A. Habibi-Yangjeh and S. Rahim Pouran, *J. Ind. Eng. Chem.* **2018**, 62, 125.
4. W. A. Smith, I. D. Sharp, N. C. Strandwitz and J. Bisquert, *Energy Environ. Sci.* **2015**, 8, 2851-2862.
5. A. R. Zanatta, *Sci. Rep.* **2019**, 9, 11225.
6. L. Qiao, H. Y. Xiao, H. M. Meyer, J. N. Sun, C. M. Rouleau, A. A. Paretzky, D. B. Geohegan, I. N. Ivanov, M. Yoon, W. J. Weber, M. D. Biegalski, *J. Mater. Chem. C* **2013**, 1, 4628;
7. Seki, Munetoshi. "Bandgap-Engineered Iron Oxides for Solar Energy Harvesting" In *Iron Ores and Iron Oxide Materials*, edited by Volodymyr Shatokha. London: IntechOpen, **2018**. 10.5772/intechopen.73227;
8. H. Mashiko, T. Oshima, A. Ohtomo, *Appl. Phys. Lett.* **2011**, 99, 241904;
9. T. J. Smart, T. A. Pham, Y. Ping, T. Ogitsu, *Phys. Rev. Mater.* **2019**, 3, 102401.
10. G. Kresse and J. Furthmüller, *Phys. Rev. B* **1996**, 54, 11169-11186.
11. P. E. Blöchl, *Phys. Rev. B* **1994**, 50, 17953-17979.
12. J. P. Perdew, K. Burke and M. Ernzerhof, *Phys. Rev. Lett.* **1996**, 77, 3865-3868.
13. a) D. Vernekar, M. Dayyan, S. Ratha, C. V. Rode, M. A. Haider, T. S. Khan and D. Jagadeesan, *ACS Catal.* **2021**, 11, 10754-10766;
14. B. Zhang, X. Zheng, O. Voznyy, R. Comin, M. Bajdich, M. García-Melchor, L. Han, J. Xu, M. Liu, L. Zheng, F. P. G. d. Arquer, C. T. Dinh, F. Fan, M. Yuan, E. Yassitepe, N. Chen, T. Regier, P. Liu, Y. Li, P. D. Luna, A. Janmohamed, H. L. Xin, H. Yang, A. Vojvodic and E. H. Sargent, *Science* **2016**, 352, 333-337.

15. A. Jain, S. P. Ong, G. Hautier, W. Chen, W. D. Richards, S. Dacek, S. Cholia, D. Gunter, D. Skinner, G. Ceder and K. A. Persson, *APL Materials* **2013**, 1, 011002.
16. C. P. Plaisance and R. A. van Santen, *J. Am. Chem. Soc.* **2015**, 137, 14660-14672.
17. H. J. Monkhorst and J. D. Pack, *Phys. Rev. B*, **1976**, 13, 5188-5192.